Electronic Supplementary Material (ESI) for Soft Matter.
This journal is © The Royal Society of Chemistry 2018

Supplementary Information

Entangled Chain Polymer Liquids Under Continuous Shear Deformation: Consequences of a Microscopically Anharmonic Confining Tube

Shi-Jie Xie[1] and Kenneth S. Schweizer[1-4,*]

Departments of Materials Science[1], Chemistry[2], Chemical & Biomolecular Engineering[3], and Frederick Seitz Materials Research Laboratory[4], University of Illinois, 1304 West Green Street, Urbana, IL 61801, USA

*kschweiz@illinois.edu

Derivation of the Microscopic Force Projection Factor

The "projection factor" $\sqrt{1-S^{3/2}}/2$ in Eq.(6) is derived as follows. If the imposed deformation tensor is $\vec{\vec{E}}$ then the required PP step orientational distribution function is [1]

$$g\left(\vec{u}_i,\vec{\vec{E}}\right)=\frac{1}{4\pi\left\langle\left|\vec{\vec{E}}\cdot\vec{u}'\right|\right\rangle_0}\int d\vec{u}'\left|\vec{\vec{E}}\cdot\vec{u}'\right|\delta\left(\vec{u}_i-\frac{\vec{\vec{E}}\cdot\vec{u}'}{\left|\vec{\vec{E}}\cdot\vec{u}'\right|}\right) \tag{S1}$$

where $\left\langle\cdots\right\rangle_0=\int d\vec{u}'/4\pi$ is the average over an isotropic distribution of orientations and $\vec{u}'$ and $\vec{u}_i$ are unit vectors before and after deformation, respectively. Eq. (S1) implies the probability that an arbitrarily chosen point of the deformed PP step is in the direction of $\vec{u}_i=\vec{\vec{E}}\cdot\vec{u}'/\left|\vec{\vec{E}}\cdot\vec{u}'\right|$ is proportional to $\left|\vec{\vec{E}}\cdot\vec{u}'\right|$ [1]. For a shear deformation, $\vec{\vec{E}}$ is [1]

$$\overleftrightarrow{E}_{shear}=\begin{pmatrix}1 & \gamma & 0\\ 0 & 1 & 0\\ 0 & 0 & 1\end{pmatrix} \tag{S2}$$

The inset of Figure A1 defines the unit vector of the PP step $\vec{f}_{\parallel}\left(\theta_1,\varphi_1\right)$, tube diameter (perpendicular to PP step axis) $\vec{f}_{\perp}\left(\theta_2,\varphi_2\right)$, and shear direction $\vec{f}\left(1,0,0\right)$ in our calculation. The PP step unit vector can be written as

$$\vec{f}_{\parallel}=\frac{\vec{\vec{E}}\cdot\vec{u}'}{\left|\vec{\vec{E}}\cdot\vec{u}'\right|} \tag{S3}$$

The angle between the vector perpendicular to the PP step axis and lab shear direction is defined as $\theta_{\perp}$ (inset of Fig.A1). Hence, $\left\langle\left|\cos\left(\theta_{\perp}\right)\right|\right\rangle$ quantifies the component of external force orthogonal to the PP axis, which follows from Eqs. (S3) - (S6) as:

$$\left\langle\left|\cos\theta_{\perp}\right|\right\rangle=\int_0^{\pi}d\theta_1\int_0^{2\pi}d\varphi_1\int_0^{\pi}d\theta_2\int_0^{2\pi}d\varphi_2\sin\theta_1\sin\theta_2\delta\left(\theta_2-\theta_2'\right)\left|\cos\theta_{\perp}\right|g\left(\vec{f}_{\parallel}\left(\theta_1,\varphi_1\right),\vec{E}\right) \tag{S4}$$

$$\cos\theta_{\perp}=\frac{\vec{f}\cdot\vec{f}_{\perp}\left(\theta_2,\varphi_2\right)}{\left|\vec{f}\right|\cdot\left|\vec{f}_{\perp}\left(\theta_2,\varphi_2\right)\right|} \tag{S5}$$

$$\theta_2'=\arctan\left(\frac{-\cot\theta_1}{\cos\varphi_1\cos\varphi_2+\gamma\sin\varphi_1\cos\varphi_2+\sin\varphi_1\sin\varphi_2}\right) \tag{S6}$$

We assume the PP step orientation is induced by an affine step shear deformation of amplitude γ. The associated degree of orientational order is then given by Eq. (17).

Figure S1 presents the calculated $\left\langle\left|\cos\left(\theta_{\perp}\right)\right|\right\rangle$ as a function of the orientational order parameter S. As expected, $\left\langle\left|\cos\left(\theta_{\perp}\right)\right|\right\rangle$ monotonically decreases with S, implying the effect of the direct stress-dependent force on dynamic free energy F_{dyn} becomes weaker due to PP step orientation. For simplicity, an accurate analytic expression $\sqrt{1-S^{3/2}}/2$ (green dashed line in Figure S1) is used in the numerical calculations reported in the text.

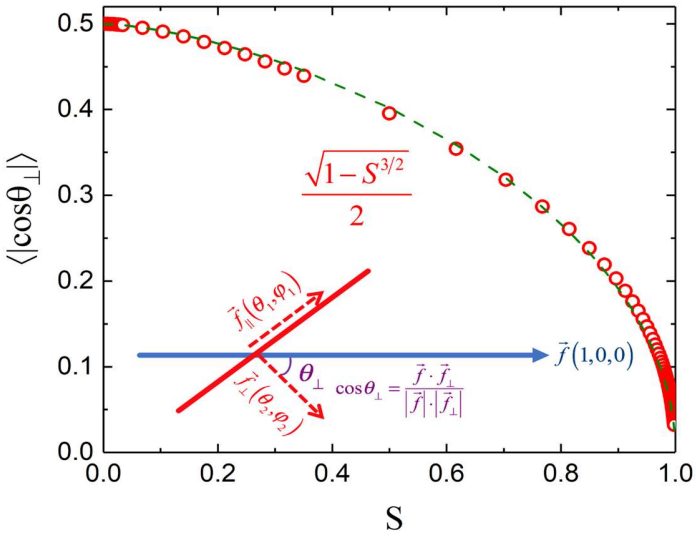

Figure S1 Red circles are $\left\langle\left|\cos\left(\theta_{\perp}\right)\right|\right\rangle$ values as a function of the PP step orientational order parameter S . The green dashed curve is the "projection factor" used in the main text. Inset: Schematic diagram for the unit vector of the PP step $\vec{f}_{\parallel}\left(\theta_1,\varphi_1\right)$, tube diameter direction (perpendicular to the axis of a PP step) $\vec{f}_{\perp}\left(\theta_2,\varphi_2\right)$, and shear direction $\vec{f}\left(1,0,0\right)$. The angles $\left(\theta_1,\varphi_1\right)$ and $\left(\theta_2,\varphi_2\right)$ are spherical coordinates for unit vectors $\vec{f}_{\parallel}$ and $\vec{f}_{\perp}$, respectively.

Details of Rheological Theory of Continuous Startup Shear Deformation

Model Constitutive Equation

We adopt the simplest version of the Mead-Larson-Doi (MLD) model [2] as the constitutive equation framework. The chain PP contour length stretch ratio $\lambda(t) \equiv l_{PP}(t) / l_{PP,0}$ describes in an average sense any PP step on any chain. The basic rheological equations are [2]:

$$\sigma\left(t\right) = 5G_e\lambda\left(t\right)^2 S_{xy} \tag{S7}$$

$$S_{xy} = \int_{-\infty}^{t} dt' \frac{d\psi\left(t-t'\right)}{dt'} Q_{xy}\left[E\left(t,t'\right)\right] \tag{S8}$$

where S_{xy} is the xy-component the orientation tensor, G_e is the plateau shear modulus, $Q_{xy}\left(z\right) \approx z/\left(5+z^2\right)$ is the affine deformation orientational factor [1], E is the accumulated deformation, and the tube survival function is the accumulated orientational relaxation associated with an effective orientational relaxation time τ_{eff} :

$$\psi\left(t-t'\right)=\exp\left(-\int_{t'}^{t}dt''\tau_{eff}^{-1}\left(t''\right)\right) \tag{S9}$$

which includes (perturbed) reptation, CCR and perhaps activated transverse entropic barrier hopping (see section III.E). Recent simulations [3] found the factorization of total stress into orientational and stretch contributions per Eq.(S7) is quite accurate.

Delayed Onset of Chain Retraction

Based on the dynamic tension blob concept [4,5], we recently formulated [6] a theoretical description of the so-called interchain "grip force" f_{grip} [7] envisioned as the microscopic origin of affine stretching of the PP contour length in entangled liquids. We found that f_{grip} has distinctive strain-dependences under continuous shear deformation [6]. The corresponding intrachain retraction force $f_{retract}$ can be obtained based on a microrheological perspective [6], and linearly increases with strain.

The key physical idea (per Wang et al. [7]) is that as long as f_{grip} is stronger than $f_{retract}$, polymers stretch in a purely elastic affine manner. But once the retraction force exceeds the grip force, it becomes possible for chain retraction to commence, which signals the breakdown of affine deformation of the PP contour length. The force imbalance criterion follows by equating the grip and retraction forces to obtain the mean "loss of grip" strain, γ_{grip} . For Wi_R <1 we found [6] $\gamma_{grip}\approx 1.8\sqrt{Wi_R}$, which is well below the DE model [1] value of ~2.25 for the stress overshoot strain. For Wi_R>1 we derived [6] $\gamma_{grip}\approx 2.3\,Wi_R^{1/3}$. The 1/3 exponent arises from a competition between the strain dependences of the grip and retraction forces, and agrees well with the 1/3 power

law for the overshoot strain ($\gamma_{\max} \approx 2Wi_R^{1/3}$) found in experiments [7] and simulation [8]. But a convincing analysis requires a full rheological calculation [6].

Consequences of Tube Diameter Fluctuations

The anharmonic tube confinement potential of Section II implies the existence of a broad distribution of tube diameters, in the spirit of simulation-based PP analyses [9,10]. Such tube diameter fluctuations modify the entanglement strand retraction force strength via the conversion step from elastic stress to microscopic force [6,11], and imply a distribution of force imbalance conditions and loss of grip strains, $P\left(\gamma_{grip}\right)$. The fraction of strands that have achieved force imbalance at a given strain is [6,11]

$$\Theta_{grip}\left(\gamma\right) = \int_0^{\gamma} P\left(\gamma_{grip}\right) d\gamma_{grip} \tag{S10}$$

This function broadens with shear rate mainly due to a shift of the most probable value of γ_{grip}. With increasing strain there is a continuous loss of grip and crossover from solid-like to liquid-like response of the chain stretch degree of freedom.

Chain Stretch Dynamics

The chain-level PP contour length degree of stretch, λ, is described in a globally mean fashion corresponding to an average over entanglement strands on any specific chain and all chains in the system. Based on our physical picture, we postulated the following evolution equation for PP contour length stretch [6,11]:

$$\frac{d\lambda}{dt} = S_{xy}\dot{\gamma}\,\lambda - \frac{\lambda - 1}{\tau_{R,eff}}\Theta_{grip}\left(\gamma\right) \tag{S11}$$

The first term describes affine stretching in the standard manner [2,12]. The second term describing retraction has two qualitatively new elements. First, it continuously "turns on"

from zero with increasing elapsed time or accumulated strain thereby capturing the amount of loss of grip (as quantified by $\Theta_{grip}(\gamma)$). Second, as grip is lost the PP contour length increasingly behaves in an unentangled manner. Retraction is faster when $Wi_R>1$ because Rouse modes of wavelength larger than ξ do not dissipate energy [5]. Here ξ is the scale below which a polymer remains conformationally equilibrated and beyond which it stretches [5]. The effective retraction time decreases as [5] $\tau_{R,eff}(\dot{\gamma}) \propto \tau_{R,0}\,\xi / R_{ee}$ and quantitatively:

$$\tau_{R,eff}(\dot{\gamma}) = \frac{\eta(\dot{\gamma})}{G_{Rouse}} = \frac{\tau_R}{\left[1+Wi_R^2\right]^{1/4}} \tag{S12}$$

where the final equality is an accurate interpolation formula [5].

Effective Orientational Relaxation and Barrier Hopping Times

The analogous results of Fig.5 for a larger Z=25 are given below. All trends are the same as found for Z=6.

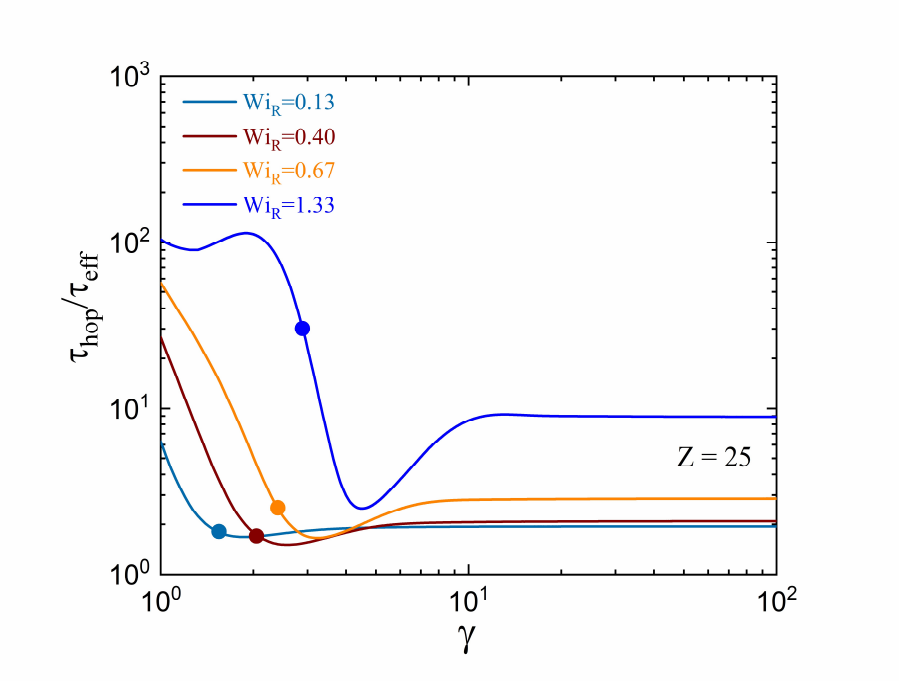

Figure S2 Log-log plot of the transverse barrier hopping time normalized by the effective orientational relaxation time as a function of strain for Z=25 and four low shear rates. Dots indicate the strains at the stress overshoot.

Orientational Order Parameter at the Stress Overshoot

The analogous results of Fig.6 for the nematic orientational PP step order parameter but at the stress overshoot are given below. All trends are qualitatively the same as found in the steady state.

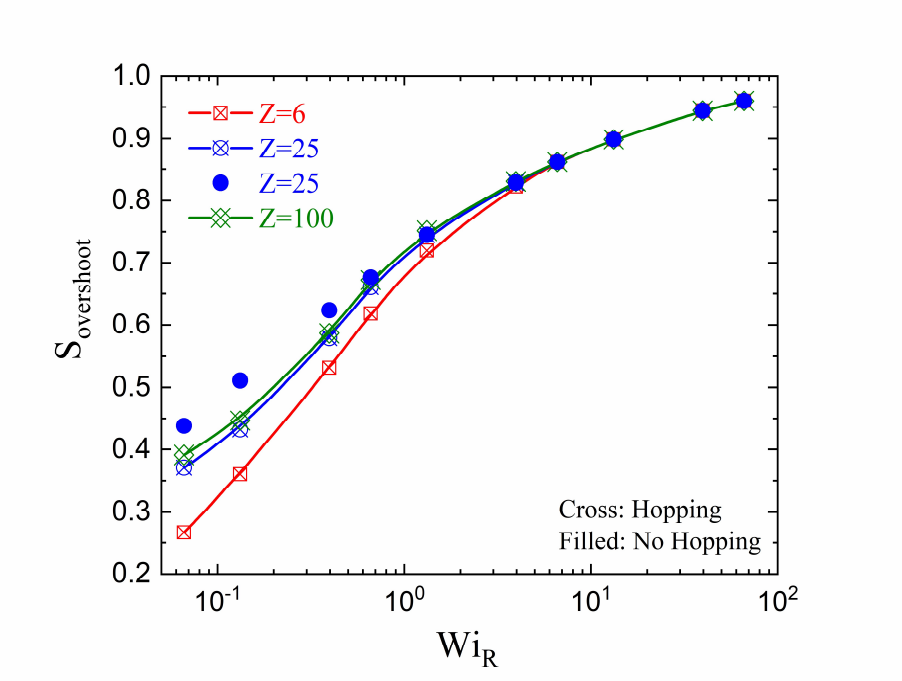

Figure S3 PP step nematic orientational order parameter at the stress overshoot as a function of Rouse Weissenberg number for weakly entangled ($Z = 6$) to heavily entangled ($Z = 100$) melts. Cross and filled symbols are results with the hopping process (Eq. (15)) and without hopping process (Eq. (14)), respectively.

Dynamic Tube Diameter at the Stress Overshoot

The analogous results of Fig.7 for the dynamic tube diameter at the stress overshoot are given below. All qualitative trends are the same as found in steady state.

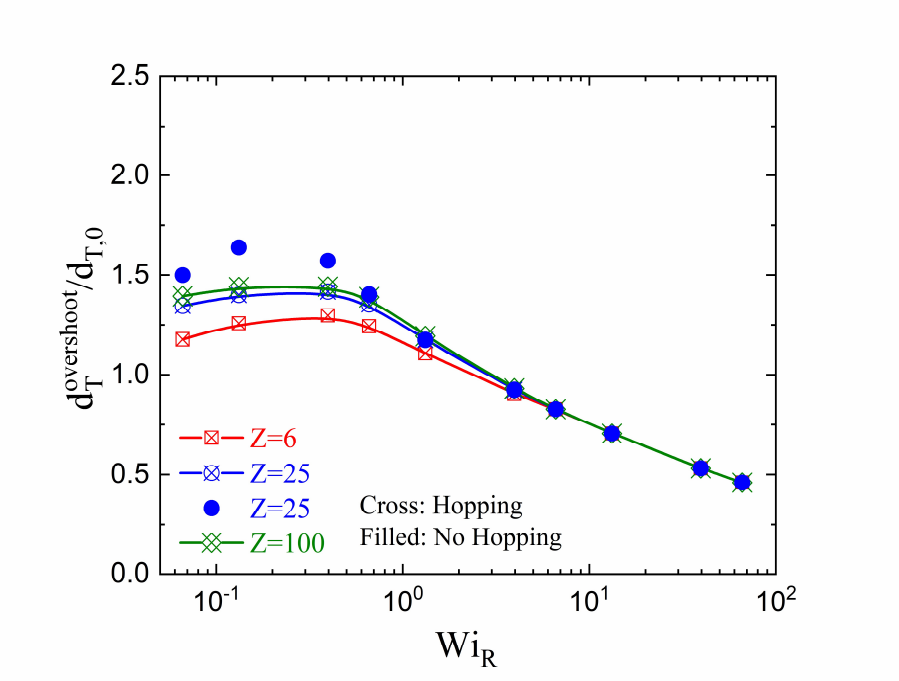

Figure S4 The normalized tube diameter at the stress overshoot as a function of Rouse Weissenberg number for weakly entangled ($Z = 6$) to heavily entangled ($Z = 100$) melts. Cross symbols are results with hopping (Eq. (15) and filled symbols ignore hopping (Eq. (14).

Flow Curve

As relevant background to discuss the steady state behavior of the transverse barrier, Figure S5 shows our results (including hopping for computing τ_{eff}) for the flow curve for four degrees of entanglement which span the weakly to heavily entangled range, Z=5, 15, 25, 45. An example for Z=45 is also shown that does not include hopping, and one sees it does not matter. The flow curves are all monotonic with shear rate. For slow nonlinear deformations, the usual expansion of the width and flattening of the intermediate plateau-like regime is predicted with increasing Z.

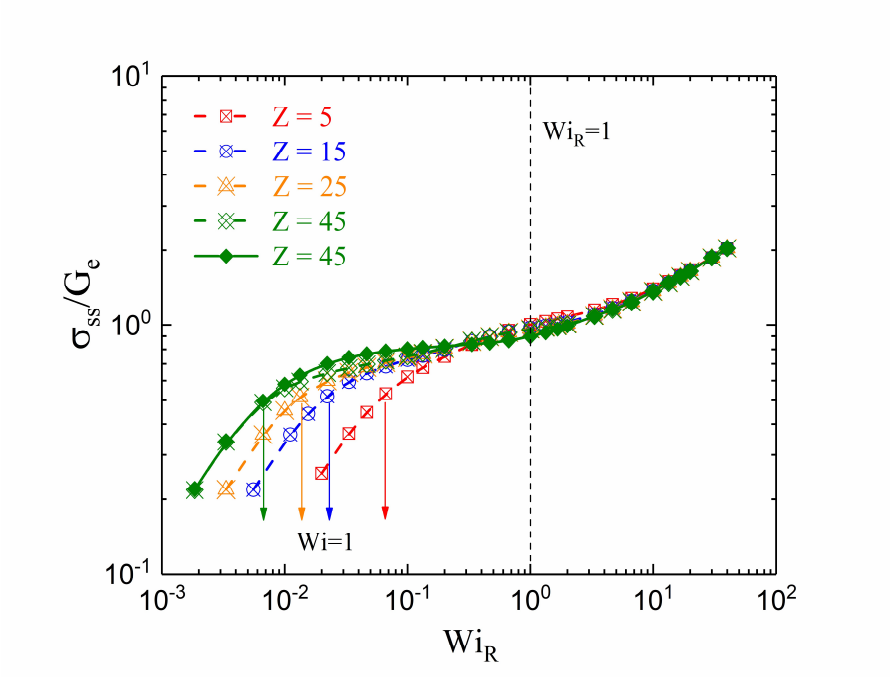

Figure S5 Dimensionless steady state flow stress versus Rouse Weissenberg number for Z=5, 15, 25 and 45. Cross symbols represent results where transverse barrier hopping in the calculation of the effective orientational relaxation time; one example of not including hopping is shown for Z=45 (solid diamonds). Curves are a guide to the eye. The onset of the nonlinear regime at Wi=1 is indicated by the arrows.

References

(1) M. Doi and S. F. Edwards, *The Theory of Polymer Dynamics*, Clarendon Press, Oxford, 1986.

(2) D. W. Mead, R. G. Larson and M. Doi, *Macromolecules*, 1998, **31**, 7895.

(3) M. H. N. Sefiddashti, B. J. Edwards and B. Khomami, *Phys. Rev. Fluids*, 2017, **2**, 083301.

(4) M. Rubinstein and R. H. Colby, Polymer Physics, Oxford Univ. Press: New York,

2003.

(5) R. H. Colby, D. C. Boris, W. E. Krause and S. Dou, *Rheol. Acta*, 2007, **46**, 569.

(6) K. S. Schweizer and S.-J. Xie, *ACS Macro Lett.*, 2018, **7**, 218.

(7) S.-Q. Wang, *Nonlinear Polymer Rheology: Macroscopic Phenomenology and Molecular Foundation*, Wiley, Hoboken, NJ, 2018.

(8) J. Cao and A. E. Likhtman, *ACS Macro Lett.*, 2015, **4**, 1376.

(9) D. M. Sussman and K. S. Schweizer, *Phys. Rev. Lett.*, 2012, **109**, 168306.

(10) C. Tzoumanekas and D. N. Theodorou, *Macromolecules*, 2006, **39**, 4592.

(11) S.-J. Xie and K. S. Schweizer, *Macromolecules*, 2018, **51**, 4185.

(12) D. S. Pearson, A. D. Kiss, L. J. Fetters and M. Doi, *J. Rheol.* 1989, **33**, 517.